PLA/PHBV Films with Improved Mechanical and Gas Barrier Properties

Majdi Boufarguine, Alain Guinault, Guillaume Miquelard-Garnier,* Cyrille Sollogoub*

Blending poly(lactic acid) (PLA) with a small amount of poly(3-hydroxybutyrate-*co*-3-hydroxyvalerate) (PHBV; 10 wt%) using a custom multilayer co-extrusion process increases both ductility and gas barrier properties of extruded films compared with neat PLA and classical blending methods. The co-extrusion process allows multiplication of the number of alternate layers of PLA and PHBV within a film. It was observed that for a critical number of theoretical layers, PHBV layers are broken into lamellas. A well-developed lamellar morphology, with thin and long lamellas of highly crystalline PHBV in PLA matrix was obtained. A balance between aspect ratio and crystallinity of the lamellas, and their dispersion within the PLA matrix was needed to obtain films with improved permeability and mechanical properties.

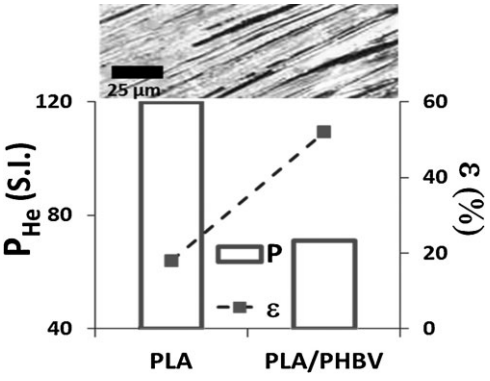

1. Introduction

Recently, environmental concerns and disruptions of oil resources have led to increased efforts in the use of biodegradable polymers at an industrial scale, especially in food packaging. For example, the use of poly(lactic acid) (PLA) is motivated by an acceptable balance between advantages and limitations of this biosourced polymer.[1–4] In particular, PLA has good transparency, and some of its mechanical properties (such as Young's modulus) are similar or even better than those of the most used polymers in packaging industries (polyolefins, PET, PS). Its relatively low glass transition and melting temperatures make it also interesting in terms of processing. However, the main limitations of PLA as a packaging material are a high gas permeability (CO_2, O_2, and water vapor) and a low ductility.[1–4]

Dr. G. Miquelard-Garnier, Dr. C. Sollogoub, Dr. M. Boufarguine, Dr. A. Guinault
P-2AM, CNAM, 292, rue Saint-Martin, 75003 Paris, France/PIMM, Arts et Métiers ParisTech, 151, Bd de l'Hôpital, 75013 Paris, France
E-mail: guillaume.miquelard_garnier@cnam.fr; cyrille.sollogoub@cnam.fr

Recent work has been done to improve these limitations; especially, a first structural way to improve barrier properties of PLA consists in increasing its crystallinity. For example, work by Guinault et al.[5,6] on cold crystallization and stereochemistry of the PLA showed that, after exceeding a crystallinity degree of approximately 40%, gas permeability decreases by a factor of about two for oxygen and three for helium. However, the authors showed[6] that recrystallization led to significant decrease of elongation at break of PLA films.

Another solution widely explored[2] to improve the gas barrier properties of the PLA is to increase the pathway length of gas molecules incorporating nanofillers. In particular, inorganic fillers like talc or clay based nanoparticles presenting high aspect ratio, have been widely used to decrease the gas barrier permeabilities of PLA due to a tortuosity effect. The permeability reduction depends on the amount, size, and dispersion state of fillers but classically, a decrease by a factor of two to four was found with incorporation of 10–15 wt% of nanoclays.[7,8] This tortuosity effect can be advantageously combined with a nucleation effect of the fillers, allowing to reach a factor-two reduction with less than 5 wt% of particles.[9] Unfortunately, these nanocomposites exhibited enhance-

ment in modulus along with a decrease of tensile strength and elongation at break.[7,10,11] Besides, several works reported an accelerated ageing and degradation of PLA-nanofillers composites.[12,13]

Finally, blending PLA with another polymer may be a simple strategy to combine performance of the two species.[2,14] Indeed, combining PLA with other biodegradable polymer like polycaprolactone (PCL),[15] polybutylene succinate (PBS),[16] or polyhydroxylalkanoates (PHA)[17,18] can be an alternative to the two first methods to bypass PLA limitations without losing the biodegradable and/or the bio-based feature of the final product.

For example, blending PLA with polyhydroxybutyrate (PHB), a highly crystalline biopolymer with high melting point and among the most studied PHAs, leads to materials with interesting physical, thermal, and mechanical properties compared to neat PLA.[17,19,20] Zhang et al.[19,20] showed an improvement of tensile properties for PLA/PHB 75/25 blend due to reinforcement effect of the small finely dispersed PHB particles. They found that the addition of PHB significantly improves the crystallinity and crystallization rate of PLA. Similarly, Noda et al.[17] found an improvement in toughness of PLA/PHAs (Nodax) blends, as long as the content of included PHAs is not too high (below 20 wt%). This singular behavior was explained by unusually slow crystallization kinetics of PHAs, when PHAs particles are dispersed in small domains (around 1 μm), leading to rubbery amorphous PHAs particles dispersed in hard and brittle PLA matrix.

Nevertheless, thermal degradation, brittleness, and low ductility of PHB make this bio-polyester very difficult to process and not suitable for several applications. These properties can be improved by the synthesis of linear random copolymers of PHB and chemically similar units modified with alkyl dangling chains which are more flexible. For example, poly(3-hydroxybutyrate-*co*-3-hydroxyvalerate) (PHBV) is a commercially available copolymer containing segments of 3-hydroxybutyrate (HB) group and 3-hydroxyvalerate (HV) groups (lateral ethyl group instead of a methyl group) alternated randomly (Figure 1). As the fraction of HV groups increases in the chain, the copolymer shows a decrease in the Young's modulus along with an increase of the elongation at break, with a rather sharp transition, from brittle to ductile behavior, around 10 mol% HV.[21–23] This incorporation leads to a lowering of both the crystallinity and the melting temperatures.[21,22] The lower melting point of the copolymers compared to that of PHB leads to a wider process window.

Several authors[24–28] focused on the PLA/PHBV blends especially to improve ductility of commercial PLA with high molecular weight (Mw typically >200 000 $g \cdot mol^{-1}$). When both polymers have a high molecular weight, all the blends were found immiscible. The PHBVs used in these studies were all different (with different fractions of HV groups), which explains the wide variety of mechanical properties obtained for PLA/PHBV blends. In most studies however, it was found that blending PLA and PHBV can lead, for some compositions, to improved mechanical properties. Nanda et al.,[27] e.g., observed that while the tensile modulus followed a classical mixing rule, elongation at break of their blends was dramatically increased and systematically more than that of neat polymers (in their case, compositions studied were PHBV/PLA 50:50, 60:40, and 70:30 wt%), even though the mechanism responsible for this result is not addressed. Same trends were observed by Pivsa-Art et al.,[29] this time on fibers from PLA/PHBV blends with 5 wt% of PHBV. Wang et al.[28] showed that the addition of poly(ethylene glycol) in PDLLA/PHBV blends significantly increases the impact strength and elongation at break. Recently, Gerard and Budtova[25] insisted on the importance of the blend morphology on the properties of the final blends. They observed a nodular morphology for blends containing <30 wt% of one component and pointed out a peculiar morphology obtained for PLA/PHBV (90/10), e.g., a very small dispersion of PHBV droplets of about 400 nm within the PLA matrix.

Even if no attention has been given to the gas barrier properties of PLA/PHBV blends, PHBV appears also as a good candidate to decrease PLA permeability, since it presents significantly better gas barrier properties than PLA[22] (water vapor: $P_{PLA} = 18 \times 10^{-12}\ g \cdot m \cdot m^{-2} \cdot s^{-1} \cdot Pa^{-1}$, $P_{PHBV} = 2.7 \times 10^{-12}\ g \cdot m \cdot m^{-2} \cdot s^{-1} \cdot Pa^{-1}$; Oxygen: $P_{PLA} = 2.95\ cm^3 \cdot \mu m \cdot m^{-2} \cdot d^{-1} \cdot atm^{-1}$, $P_{PHBV} = 0.26\ cm^3 \cdot \mu m \cdot m^{-2} \cdot d^{-1} \cdot atm^{-1}$).

In this work, we explored an original way to combine PLA and PHBV, using a multilayer co-extrusion setup,[30] allowing to process a film composed of alternated PLA and PHBV layers from three to theoretically several thousand layers. We compared the resulting films to ones prepared by a classic "dryblend" method of PLA and PHBV, where the two polymers are dry-blended before melt blending in a single screw extruder. This dryblend method was

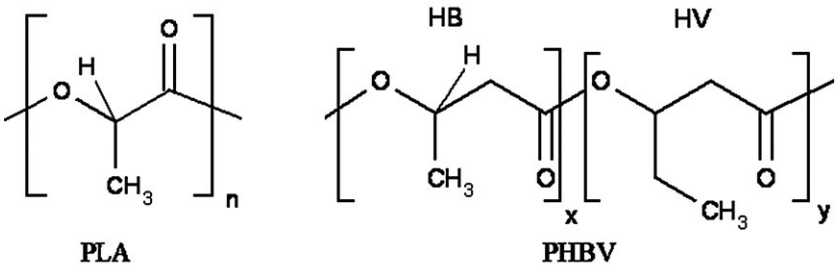

Figure 1. Chemical structure of PLA and PHBV.

used[31,32] to produce films with developed lamellar blend morphologies, well-known to offer improved gas barrier properties. The morphologies of our films have been investigated and related with the measured mechanical properties and gas permeabilities. The aim of this work was thus to gain a better understanding in the relation between blend morphologies, crystallinity, and film features (mechanicals, thermal, and barrier properties) for these promising PLA/PHBV blends, e.g., how the microstructure of the blends will affect the final properties of the material.

2. Materials and Methods

2.1. Materials

2002D PLA, an extrusion grade, was purchased from Natureworks, USA. This PLA is a Poly(D,L-lactide) with a percentage of D-lactic acid units of 4.3%.[33] Its melt temperature is close to 160 °C, with a melt index of 5–7 g/10 min as given by Natureworks. The molecular weight as determined by SEC is $\overline{M}_w \approx 210\,000\ g \cdot mol^{-1}$ with a polydispersity index PDI of 2.1. ENMAT Y1000P PHBV was obtained from Tianan Biologic, China. Y1000P is a PHBV containing 8% mol of HV groups, and $\overline{M}_w \approx 340\,000\ g \cdot mol^{-1}$ (DPI ≈ 2.5),[22] with a melt temperature close to 170 °C. The melt flow index is reported to be 2.4 g/10 min at 170 °C.[34] Both were used as received, in pellet form, but dried with desiccant air before use (4 h at 90 °C for the PHBV, 4 h at 80 °C for the PLA).

2.2. Preparation of Blends

PLA–PHBV multilayer films (3 to 2 049 theoretical layers) were extruded using a multilayer co-extrusion block connected to two single-screw extruders arranged in parallel according to a classical co-extrusion process (three-layer), using a similar device to the one developed by Baer et al.[35] 30 mm-diameter Mapre extruder was used for PLA and a 20 mm-diameter Scamex extruder for the PHBV. Extrusion temperature was set at 190 °C for both polymers to prevent degradation, because of the narrow processing conditions.

The amount of each polymer in the film was set to 90% PLA for 10% PHBV (wt%) by adjusting the screw speeds of each extruder to control the throughput. For the multilayer films prepared in this study, the Mapre screw speed was 40 rpm and the Scamex screw speed was 92 rpm (adding multiplying elements in the extrusion block does not modify significantly the final throughput).

The theoretical number of layers N_{lay} was determined by the number of multiplying elements (Figure 2) arranged in series in a multiplication block and given by Equation (1):

$$N_{lay} = 1 + 2^{N+1} \quad (1)$$

where N is the number of multiplying elements.

The dryblend films were prepared with the Mapre extruder after a mixing of PLA and PHBV pellets outside the extruder. Following some authors,[31,32] the processing conditions (screw speed and temperature) have been optimized in order to obtain a well-developed lamellar morphology. In particular, the screw speed was for these samples set at 70 rpm (with an extrusion temperature of 190 °C) in order to obtain a good balance between the residence time and the shear rate in the extruder.

For the two kinds of samples, the output film was then extruded through a flat die of 1 mm thickness and 200 mm width and then stretched and cooled with chill rolls rotating at a chosen speed. Since this speed may impact the final thickness of the film (and in consequence the cooling rate of the sample) and also apply additional deformation to the sample that can modify its microstructure, it was adjusted depending on the extrusion method to produce films with final thicknesses around 200 μm (either 2 or $4\ m \cdot min^{-1}$ for the multilayer films and fixed at $6\ m \cdot min^{-1}$ for the dryblend samples which are thicker when coming out of the extruder).

PLA and PHAs are known to age over time especially over the course of the first 2–3 weeks after film preparation, even when stored below T_g, with an increase in the Young's modulus and a decrease in the elongation at break.[22] In

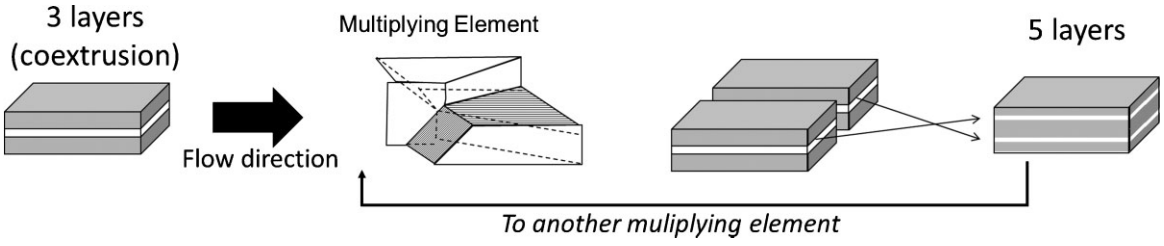

Figure 2. Schematic of the multilayer co-extrusion process.

this study, results presented were obtained on films tested several weeks after preparation (at least 2 weeks). Reproducibility was assessed by measuring the same films up to 6 months after their preparation without noticeable changes for every characterization performed.

2.3. Film Characterizations

Films mechanical properties (Young's modulus and elongation at break) were measured on an Instron 4507 with a 100 N load cell. At least five dog-bone shaped samples, with 58 mm of length and 5 mm in width, were taken in the center of the film in the extrusion direction. The deformation rate was fixed at 5 mm · min^{-1} for all samples, force and deformation were measured and stresses and strains were calculated from these measurements. For each sample, average values of elongation at break (ε_b) and Young's modulus (E, calculated by taking the initial slope of the stress–strain curves) were collected and compared.

The degrees of crystallinity (χ) of PLA and PHBV in the films were measured using a Pyris1 DSC (Perkin Elmer, France). The DSC was calibrated with indium as a reference. DSC thermogram was recorded in a nitrogen atmosphere with 10–15 mg of the films in an aluminum pan capped with a lid using a Perkin Elmer hand press. If necessary, several portions of films were superposed in the pan to reach a sample weight close to 10 mg. The melting temperatures were determined during the heating stage from 0 to 200 °C, at 10 °C · min^{-1}. In order to avoid any structure modification, the glass transition temperatures were determined also from this heating stage, even if the relaxation peak is present. χ was calculated using the following relation:

$$\chi = \frac{\Delta H_m - \Delta H_{cc}}{m\Delta H_{m\text{-}100\%}} \times 100\,[\%] \quad (2)$$

where ΔH_m is the melting enthalpy; ΔH_{cc} is the cold crystallization enthalpy; m is the weight fraction of the polymer, and $\Delta H_{m\text{-}100\%}$ is the melting enthalpy of totally crystallized polymer equal to 93 J · g^{-1}[4,36] for PLA and 109 J · g^{-1}[37] for PHBV. The reported values are averages of at least two samples.

Helium permeability was measured by a specific homemade analyzer at room temperature and 0% RH, based on the ISO 15105-2:2003 method. Circular portions cut from the films (surface = 23.75 cm^2) were inserted between two hermetically sealed compartments drained using nitrogen. An helium constant flow (80 mL · min^{-1}) was introduced in the upstream part of the cell and is measured in the downstream part, using an helium detector (mass spectrometer). Permeability was determined from the transmission rate by taking into account the average thicknesses of the films (average calculated by measuring the thickness on at least 9 points of the film). For assessing reproducibility of permeability, measurements were carried out on at least two different samples obtained from the same film.

Optical micrographs were obtained on samples with 10 μm thickness prepared with a Leica RM2255 microtome after immersion in liquid Nitrogen, cut perpendicular to the extrusion direction throughout the film thickness. These samples were observed using an Olympus BH2-UMA transmission microscope with two different magnifications (20× and 5×) equipped with a Leica camera. The obtained contrast by polarized light between the two phases allowed revealing the morphology of this type of blend. The dark phase corresponds to PHBV and the bright one to PLA. Pictures were then analyzed using ImageJ, an open source image processing program developed at the National Institutes of Health. Pictures were converted to binary frames to measure the average lengths and thicknesses of PHBV structures (lamellas or layers).

3. Results

3.1. Morphology

Figure 3 shows micrographs of various PLA/PHBV films: Figure 3a shows a classical three-layer co-extrusion with one central layer of PHBV; Figure 3b illustrates a film of 17 layers obtained with 3 multiplying elements. In these two films, PHBV phase appears as continuous layers. Using 6 or 10 multiplying elements should lead to films with 129 and 2049 theoretical layers, respectively. In these cases, however, we can observe that the PHBV layers appear discontinuous and more "lamellar-like" (Figure 3c–f). Lamellar structures formed are similar but slightly thinner and shorter for films with 2049 layers (definitions and value of mean thicknesses and lengths for the different films are given in Figure 4). We notice thus that increasing the number of layers leads to layers breakup and film structures similar to the ones obtained by the dryblend method (Figure 3g and h). However, in the dryblend films, lamellas are not so well dispersed as for the multilayer method and some nodules of PHBV are observed along with the lamellas.

Since the weight fraction of the PHBV is constant in our samples and assuming continuous layers, the mean thickness e_{mean} of PHBV structures created by multiplying the layers should decrease with increasing N, the number of multiplying elements, following a power law derived from Equation (1) (Equation 3).

$$e_{mean} = \frac{0.1\,e_0}{(N_{lay} - 1)/2} = \frac{0.1\,e_0}{2^N} \quad (3)$$

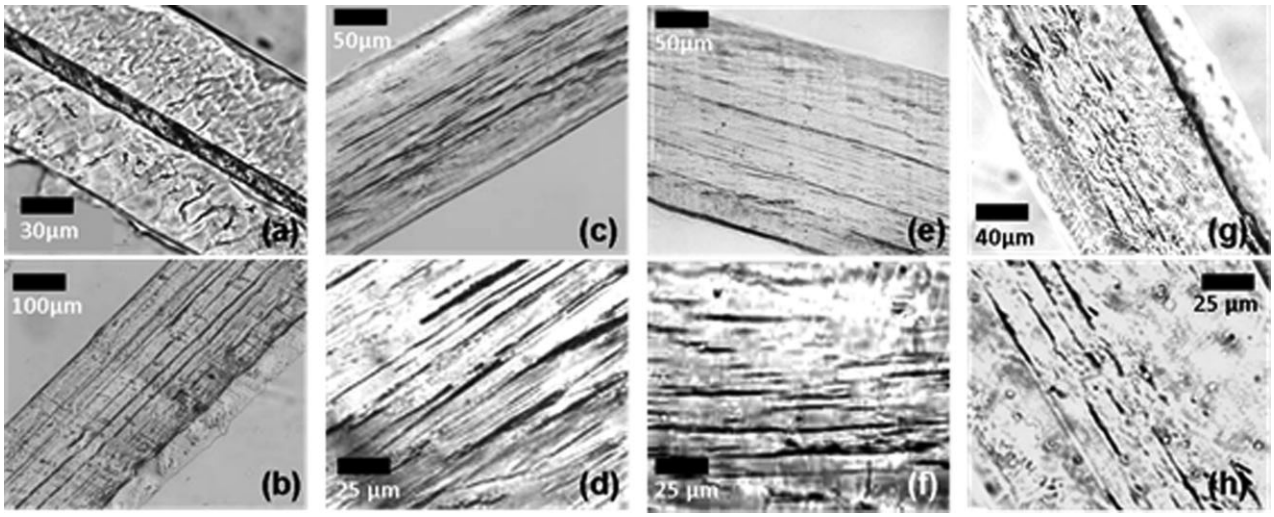

Figure 3. Optical micrographs of extruded films (a) 3 layers, (b) 17 layers, (c)(d: zoom) 129 layers, (e)(f: zoom) 2049 layers, and (g)(h: zoom) dryblend film.

where e_0 is the thickness of the film (taken as 200 µm here) and 0.1 is the proportion of PHBV within the sample.

In Figure 4, the mean thickness e_{mean} and mean length l_{mean} were estimated for all samples produced, using ImageJ analysis on the optical images, and plotted as a function of the number of multiplying elements. The mean thickness was then compared to the theoretical thickness calculated as described above. The solid line represents the theoretical thickness evolution calculated with the targeted initial thickness of 200 µm, whereas the hollow symbols take into account the actual mean thickness of each sample. As can be seen from the graph, good agreement is only observed for a small number of multiplying elements (hence small number of layers): significant deviation occurs somewhere between 3 and 6 multiplying elements, so for around 50 theoretical layers. This could be explained by the breakup of layers into discontinuous lamellas, previously observed with this multiplying device.[30] Indeed, for films with 129 and 2049 theoretical layers the measured thickness is always higher than the theoretical value and appears to reach a minimal critical thickness of around 2 µm, close to the mean experimental value obtained for the film produced using the dryblend method.

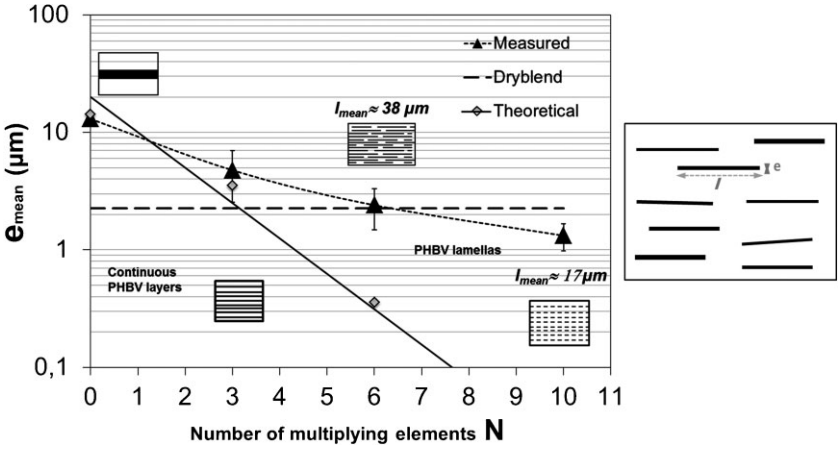

Figure 4. Comparing measured (for multilayer and dryblend films) and theoretical thickness of PHBV layers and lamellas (left). Schematic illustrating the dimensions of the lamellas (length *l*, thickness *e*) (right). The mean values are calculated by measuring the dimensions for all the lamellas within a picture.

3.2. Mechanical Properties

Mechanical properties of the obtained films are also dependent on these different structures as shown in Figure 5.

First, one can observe that the modulus, compared to the one of neat PLA, was not really impacted by the addition of PHBV, excepted for the dryblend and three-layer films with a 10% increase. The average Young's modulus for neat PLA film was found to be 3.1 GPa. Values for neat PHBV could not be obtained directly in this study since it could not be extruded alone using our apparatus, and in consequence were taken from the literature,[22] on the same PHBV reference (Enmat Y1000P) with 60% crystallinity. The modulus for this polymer was reported to be close to 4 GPa in this article, with slight variations due to ageing (from 3.9 to 4.3 GPa). One could expect that blending PLA with even a small amount of PHBV should lead to some reinforcement, but a simple estimate based on a mixing rule indicates that in this case, a 100 MPa increase in the

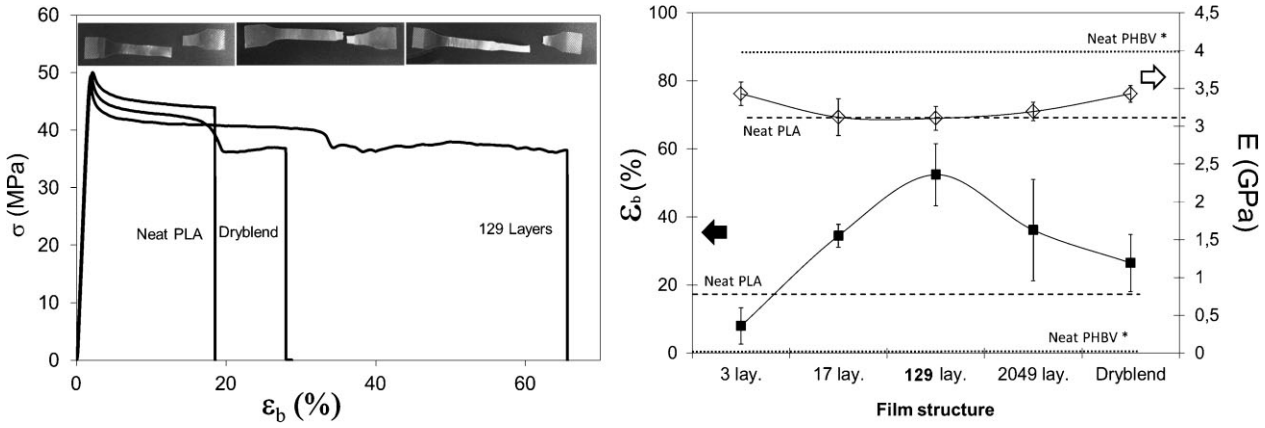

Figure 5. Evolution of the mechanical properties: typical traction curves for different films (left), elastic modulus, and elongation at break as a function of the film structure (right). Elastic modulus is shown with hollow symbols and elongation at break in full symbols. Neat PLA and neat PHBV values are in dashed lines (bottom ones for the elongation at break, top ones for the elastic moduli). *Values from neat PHBV were obtained from ref.[22]

modulus would be expected at best. The average modulus obtained for films obtained using 3, 6, and 10 multiplying elements were also 3.1 GPa, but the classical three-layer and dryblend films had a slightly higher modulus (3.4 GPa).

However the ductility changed more drastically with the blend morphology. Neat PLA film presented a quite ductile behavior in tensile test (elongation at break of 18%), quite higher than many reported work but not uncommon for measurements on extruded PLA films,[2,4] especially with the low traction speed used in this study. This ductile behavior was observed for all PLA/PHBV films (Figure 5 left). However, as expected, the three-layer film was more brittle than the neat PLA film, with an elongation at break of only 7%, because of the continuous brittle layer of PHBV which has an elongation at break of only 1% (also taken from ref.[22]). The dryblend film showed only a slight increase in the elongation at break (26%). On the contrary, for films produced using the multilayer method, one observed higher elongation at break (>35%), with a maximum for the film obtained with six multiplying elements (129 theoretical layers). For this film, the elongation at break is almost three times greater (52%) than for the neat PLA film. As shown by the picture of the sample after the tensile test (see Figure 5, left), a significant necking was observed for this sample.

3.3. Crystallinity

The DSC thermograms from the first heating run of neat PLA, PHBV, and their blends are shown in Figure 6 (left). From these curves, we can deduce the glass transition temperature (T_g), the melting point (T_m), the temperature of cold-crystallization (T_{cc}), the enthalpy of fusion (ΔH_m), the enthalpy of cold-crystallization (ΔH_{cc}), and the degree of crystallinity (χ). All these data are given in Table 1. The melting temperatures of neat PLA and neat PHBV are,

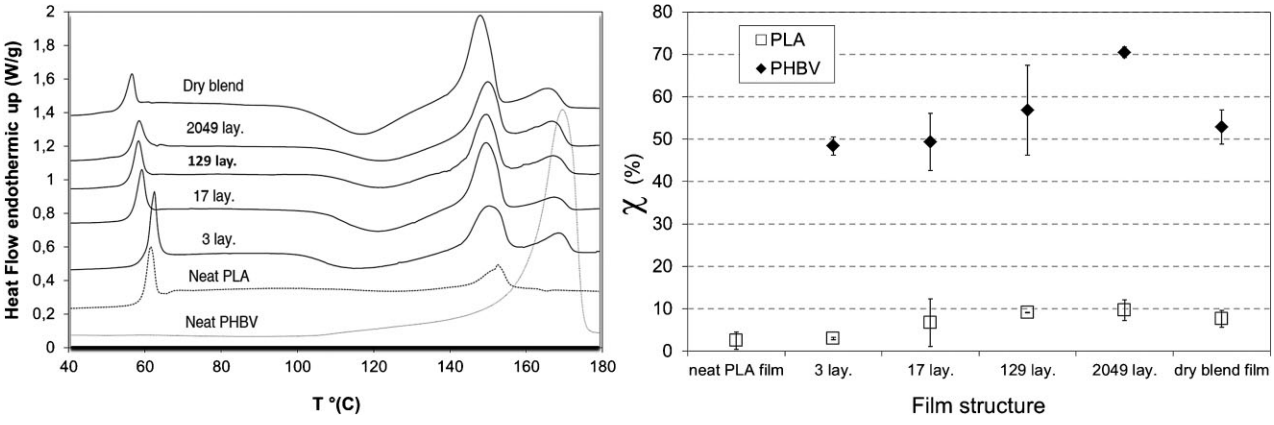

Figure 6. DSC thermograms of PLA, PHBV, and their blends (first heating run) (left) and evolution of the degree of crystallinity of PLA and PHBV in the extruded films (right).

Table 1. Detailed information obtained from differential scanning calorimetry of PLA, PHBV, and their blends.

Film Structure	T_g^{PLA} [°C]	T_m^{PLA} [°C]	T_{cc}^{PLA} [°C]	T_m^{PHBV} [°C]	ΔH_m^{PLA} [J · g^{-1}]	ΔH_{cc}^{PLA} [J · g^{-1}]	ΔH_m^{PHBV} [J · g^{-1}]
Dryblend	53	149	118	168	23.8	17.4	6.2
2049 lay.	54	150	122	167	16.8	8.6	7.7
129 lay.	55	150	123	168	15.4	7.8	6.2
17 lay.	56	150	122	169	18.3	12.6	5.4
3 lay.	59	151	124	169	13.6	11.0	5.3
Neat PLA	59	153	126	–	4.5	2.4	–

respectively, 153 and 171 °C, and remain almost constant in the blend films. On the contrary, we observe a slight decrease of the glass transition temperature of PLA from 59 °C for the neat PLA film to 54 °C for the PLA/PHBV film obtained with 10 multiplying elements. There seems to be a correlation between the decrease of T_g and the decrease of the layers/lamellas thicknesses of PHBV. This gradual decrease of the T_g of PLA phase can be understood as an increase of compatibility of PLA/PHBV blends, since the T_g of PLA shifts toward the T_g of PHBV, located at around 5 °C after Gerard and Budtova.[25] Increasing the number of layers/lamellas and decreasing their thicknesses allow to increase the interface between the two components and to improve the compatibility.

If the cold crystallization peak of PLA is very small and hardly observable in the neat PLA film, it is more pronounced in PLA/PHBV blends, especially for the dryblend film. Not only the addition of PHBV lowers the temperature of cold crystallization, but it slightly increases the degree of crystallinity of PLA (from 2% in the neat PLA film to 9%), when layer breakup appears, i.e., for more than three multiplying elements. This nucleating effect of PHBV has been already observed, when PHBV is dispersed as small nodular phase, by previous authors.[24,27] In every case, the degree of crystallinity of PLA remains extremely low (<10%).

Much more pronounced is the increase of the degree of crystallinity of PHBV as the number of layers increases: from 48% for 3 layers to 70% for 2049 layers. This result contradicts the observation of Noda et al.[17] who found that fine dispersion of PHA in PLA prevents PHA from crystallizing due to a size effect: dispersed in small discrete domains (<1 μm), the crystallization of PHA was strongly attenuated. In our case, the increase of the crystallinity as the layer thickness decreases may be attributed to strong molecular orientation induced by the polymer flow in multiplying elements. The fact that we create lamellar structure and not nodular seems to be beneficial for the crystallization of PHBV even if the thickness is small: the PHBV is not totally confined in small circular domains. In the dryblend film, where some nodules of PHBV are observed, the degree of crystallinity of PHBV is lower (about 50%).

3.4. Permeability

Since we have created a dispersion of crystallized lamellas of PHBV in PLA, there can be an interest to investigate the barrier properties of the extruded films. Measuring helium permeability rather than oxygen permeability presents several advantages: because helium molecules are smaller than oxygen, the experimental time is reduced from typically 1 day to half an hour. Moreover, helium is a neutral gas, which prevents from any possible interaction of the permeant gas within the polymer matrix.

Results are presented in Figure 7. The helium permeability showed a decrease of roughly 35% for films having one thick and continuous PHBV layer compared to neat PLA: this was simply due to the better barrier properties of the PHBV compared to the neat PLA.[24,29] Increasing the number of PHBV layers in the film, leading to a lamellar structure in the film, results in a small extra-reduction of the permeability, with a minimum (close to 40% compared to neat PLA) obtained for the film made with six multiplying elements (see Figure 7). However, it is interesting to note that the lamellar structure obtained using the dryblend

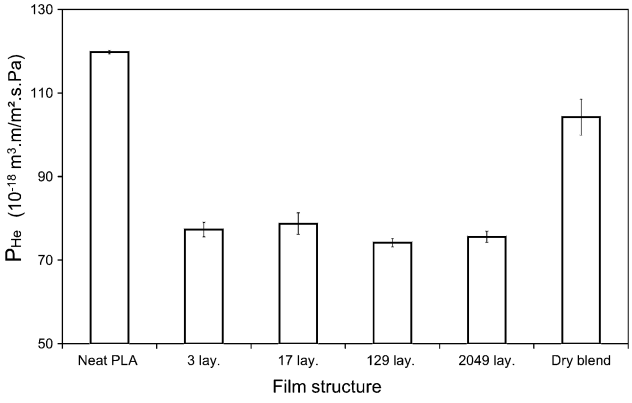

Figure 7. Helium film permeability as a function of the film microstructure.

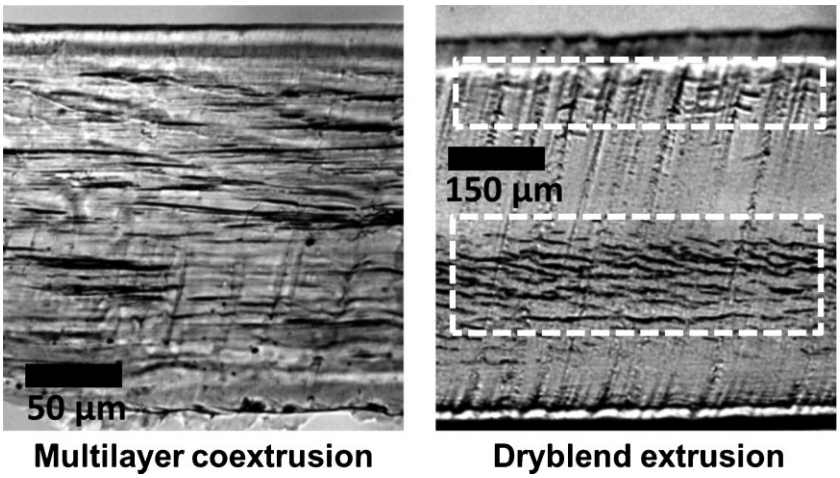

Figure 8. Dispersion of PHBV lamellas along film thickness for different films (six mixing elements on the left, dryblend on the right). Note that the dryblend presented here is thicker (same preparation method but no chill rolls), for illustration purpose.

method do not give such promising result (decrease in helium permeability <20%). This could suggest that the lamellar structure produced is not equivalent even if the sizes are comparable. This could be explained both by the presence of some PHBV nodules and by a poor distribution of the PHBV lamellas (with different crystallinities compared to the multilayer films) within the sample using the dryblend method compared to the multilayer co-extrusion method, as shown in Figure 8. In the dryblend film, lamellas are mostly localized within the white boxes, and nodules can be seen in other parts of the film (see right picture in Figure 8). In the multilayer co-extrusion film, distribution appears homogeneous at the micrometer scale.

4. Discussion

An interesting combination of results was obtained using this method on PLA blends with 10% of PHBV: Young's modulus was comparable to the PLA's one, around 3 GPa, interesting for many applications. Elongation at break and permeability which are important limitations of the PLA, were improved by a factor of 3 and 2, respectively, over neat PLA.

On the contrary, three-layer co-extrusion led to materials with improved permeability (same factor of 2) but with a lowering of the elongation at break from 18 to 8%. On the other hand, the dryblend method allowed producing materials with improved elongation at break over neat PLA (up to 26%), but the decrease of the permeability was minimal (20%).

The promising combination of the final properties could be related to the lamellar structure of PHBV and probably their good dispersion within the PLA matrix formed by multilayer co-extrusion, compared to a continuous PHBV layer (three-layer co-extrusion) or lamellas more localized at the edges of the sample (dryblend method).

The more intriguing result was the increase in the elongation at break related to the adding of PHBV, a brittle polymer, in the PLA matrix. This result has already been observed by several authors with PHBV[29,31] or other highly crystalline PHAs[17,19,20] dispersed as nodules in PLA matrix, but no universal mechanism has been proposed yet. Noda has attributed it to a prevented crystallization of PHAs when dispersed in small domains, creating "soft and deformable" regions within the material. However, this explanation could not be applied to our systems, since DSC measurements showed a high crystallinity degree for the PHBV whatever the microstructure. In our case, the observed increase of elongation at break can be attributed to the gain in compatibility when PHBV is dispersed in thin long lamellas, leading to a reduction of the T_g of PLA. This T_g reduction could be more pronounced at the interface between the PLA matrix and the PHBV lamellas, leading to softened PLA regions able to deform.

Besides, a major advantage of our films is that they can offer improved gas barrier properties: the gas permeability reduction obtained when increasing the number of layers, despite the observed layer breakup, can be attributed to the final microstructure but also to the modification of the PHBV crystallization. Indeed the permeability decrease can be related with an increase of the degree of crystallinity as observed in Figure 6 (48% for 3 layer film to 70% for 2049 layer film).

5. Conclusion

We created multilayered films of PLA/PHBV using an original multilayer co-extrusion setup. The properties of the obtained films showed that multilayer co-extrusion is a promising tool to produce blends with controlled morphology and enhanced properties over classical methods such as dryblend or three-layer co-extrusion process. In particular, PLA/PHBV (90/10 wt%) films were obtained, with a combined optimized blend morphology and crystalline structure, i.e., presenting numerous long, thin, crystallized lamellas of PHBV dispersed within the PLA matrix, with increased compatibility. The resulting films can thus combine increased elongation at break without any loss of

tensile modulus and improved gas barrier properties. Such ecofriendly films, obtained from blends of two biopolymers, show a tremendous potential for industrial use.

Acknowledgements: The authors would like to thank Ms. A. Grandmontagne, Ms. G. Dutarte, and Mr. A-S. Nguyen for helping in the preparation/characterization of some of the films presented in this study.

Keywords: barriers; biopolymers; extrusion; mechanical properties; microstructures

[1] R. Auras, B. Harte, S. Selke, *Macromol. Biosci.* **2004**, *4*, 835.
[2] L. T. Lim, R. Auras, M. Rubino, *Prog. Polym. Sci.* **2008**, *33*, 820.
[3] K. S. Anderson, K. M. Schreck, M. A. Hillmyer, *Polym. Rev.* **2008**, *48*, 85.
[4] D. Garlotta, *J. Polym. Environ.* **2001**, *9*, 63.
[5] A. Guinault, C. Sollogoub, V. Ducruet, S. Domenek, *Eur. Polym. J.* **2012**, *48*, 779.
[6] A. Guinault, C. Sollogoub, S. Domenek, A. Grandmontagne, V. Ducruet, *Int. J. Mater. Forming* **2010**, *3*, 603.
[7] J. H. Chang, Y. U. An, G. S. Sur, *J. Polym. Sci. Part B: Polym. Phys.* **2003**, *41*, 94.
[8] S. S. Ray, K. Yamada, M. Okamoto, A. Ogami, K. Ueda, *Chem. Mater.* **2003**, *15*, 1456.
[9] E. Picard, E. Espuche, R. Fulchiron, *Appl. Clay Sci.* **2011**, *53*, 58.
[10] A. Hasook, S. Tanoue, Y. Iemoto, T. Unryu, *Polym. Eng. Sci.* **2006**, *46*, 1001.
[11] G. Ozkoc, S. Kemaloglu, *J. Appl. Polym. Sci.* **2009**, *114*, 2481.
[12] H. Tsuji, Y. Kawashima, H. Takikawa, S. Tanaka, *Polymer* **2007**, *48*, 4213.
[13] S. Solarski, M. Ferreira, E. Devaux, *Polym. Degrad. Stab.* **2008**, *93*, 707.
[14] R. M. Rasal, A. V. Janorkar, D. E. Hirt, *Prog. Polym. Sci.* **2010**, *35*, 338.
[15] D. Wu, Y. Zhang, L. Yuan, M. Zhang, W. Zhou, *J. Polym. Sci. Part B: Polym. Phys.* **2010**, *48*, 756.
[16] M. Harada, T. Ohya, K. Iida, H. Hayashi, K. Hirano, H. Fukuda, *J. Appl. Polym. Sci.* **2007**, *106*, 1813.
[17] I. Noda, M. Satkowski, A. E. Dowrey, C. Marcott, *Macromol. Biosci.* **2004**, *4*, 269.
[18] Y. Takagi, R. Yasuda, M. Yamaoka, T. Yamane, *J. Appl. Polym. Sci.* **2004**, *93*, 2363.
[19] L. Zhang, C. Xiong, X. Deng, *Polymer* **1996**, *37*, 235.
[20] M. Zhang, N. L. Thomas, *Adv. Polym. Technol.* **2011**, *30*, 67.
[21] M. Avella, E. Martuscelli, M. Raimo, *J. Mater. Sci.* **2000**, *35*, 523.
[22] Y. M. Corre, S. P. Bruzaud, J. L. Audic, Y. Grohens, *Polym. Test.* **2012**, *31*, 226.
[23] S. Khanna, A. K. Srivastava, *Process Biochem.* **2005**, *40*, 607.
[24] B. M. P. Ferreira, C. A. C. Zavaglia, E. A. R. Duek, *J. Appl. Polym. Sci.* **2002**, *86*, 2898.
[25] T. Gerard, T. Budtova, *Eur. Polym. J.* **2012**, *48*, 1110.
[26] S. Modi, K. Koelling, Y. Vodovotz, *J. Appl. Polym. Sci.* **2012**, *124*, 3074.
[27] M. R. Nanda, M. Misra, A. K. Mohanty, *Macromol. Mater. Eng.* **2011**, *296*, 719.
[28] S. Wang, P. Ma, R. Wang, S. Wang, Y. Zhang, Y. Zhang, *Polym. Degrad. Stab.* **2008**, *93*, 1364.
[29] S. Pivsa-Art, N. Srisawat, N. O-Charoen, S. Pavasupree, W. Pivsa-Art, *Energy Proc.* **2011**, *9*, 589.
[30] C. Sollogoub, A. Grandmontagne, A. Guinault, "Instabilities in a Layer-Multiplying Device," in *International Conference on Advances in Materials and Processing Technologies, Pts One and Two*, Vol. 1315, F. Chinesta, Y. Chastel, M. ElMansori, Eds., Amer Inst Physics, Melville **2010**, pp. 1267–1272.
[31] P. M. Subramanian, V. Mehra, *Polym. Eng. Sci.* **1987**, *27*, 663.
[32] J. T. Yeh, S. S. Huang, W. H. Yao, *Macromol. Mater. Eng.* **2002**, *287*, 532.
[33] Y. Li, H. Wu, Y. Wang, L. Liu, L. Han, J. Wu, F. Xiang, *J. Polym. Sci. Part B: Polym. Phys.* **2010**, *48*, 520.
[34] A. Javadi, Y. Srithep, S. Pilla, C. C. Clemons, S. Gong, L. S. Turng, *Polym. Eng. Sci.* **2011**, *51*, 1815.
[35] E. Baer, J. Kerns, A. Hiltner, "Processing and properties of polymer microlayered systems," in *Structure Development during Polymer Processing*, Vol. 370, A. M. Cunha, S. Fakirov, Eds., Springer, Dordrecht **2000**, pp. 327–344.
[36] E. W. Fischer, H. J. Sterzel, G. Wegner, *Colloid Polym. Sci.* **1973**, *251*, 980.
[37] M. Scandola, M. L. Focarete, G. Adamus, W. Sikorska, I. Baranowska, S. Swierczek, M. Gnatowski, M. Kowalczuk, Z. Jedlinski, *Macromolecules* **1997**, *30*, 2568.